

1
2
3
4 **Deposition and Characterization of Diamond-like-Nanocomposite Coatings Grown by**
5
6 **Plasma Enhanced Chemical Vapor Deposition Over Different Substrate Materials**
7
8
9

10 Awadesh Kr. Mallik^{a*}; Nanadadulal Dandapat^a; Prajit Ghosh^b; Utpal Ganguly^b; Sukhendu Jana^b;
11
12 Sayan Das^b; Kaustav Guha^c; Garfield Rebello^d; Samir Kumar Lahiri^b; Someswar Datta^a
13
14

15
16 ^aCentral Glass & Ceramic Research Institute, CSIR , 196, Raja S. C. Mullick Road, Kolkata –
17
18 700032, India
19
20

21 ^bMeghnad Saha Institute of Technology, Techno India Group, Kolkata – 700107, India
22
23

24
25 ^cDepartment of Chemistry, Durham University, DH1 3LE, United Kingdom
26
27

28 ^dPerkinElmer Technology Innovation Centre, Mumbai – 400059, India
29
30

31 *Corresponding Author. Tel: +91 33 24733477. Fax: +91 33 24730957, E-mail address:
32

33
34 amallik@cgcri.res.in (A. K. Mallik)
35
36

37 **Abstract:** Diamond like Nano-composite (DLN) coatings have been deposited over different
38
39 substrates used for biomedical applications by plasma enhanced chemical vapor deposition
40
41 (PECVD). DLN has an interconnecting network of amorphous hydrogenated carbon and quartz
42
43 like oxygenated silicon. Raman spectroscopy, Fourier Transform-Infra Red (FT-IR)
44
45 spectroscopy, Transmission Electron Microscopy (TEM) and X-Ray Diffraction (XRD) have
46
47 been used for structural characterization. Typical DLN growth rate is about 1 $\mu\text{m/hr}$, measured
48
49 by stylus profilometer. Due to the presence of quartz like Si:O in the structure, it is found to have
50
51 very good adhesive property with all the substrates. The adhesion strength found to be as high as
52
53 0.6N on SS 316 L steel substrates by scratch testing method. The Young's modulus and hardness
54
55 have found to be 132 GPa and 14.4 GPa respectively. DLN coatings have wear factor in the
56
57
58
59
60
61

1
2
3
4 order of 1×10^{-7} mm³/N-m. This coating has found to be compatible with all important biomedical
5
6 substrate materials and has successfully been deposited over Co-Cr alloy based knee implant of
7
8 complex shape.
9

10
11
12 **Key words:** Diamond like-carbon; plasma CVD; coatings; tribology
13
14

15 16 **1. Introduction:** 17

18
19 Protective coatings over steel and other metals, ceramics, glasses, polymers are deposited to
20
21 increase the lifetime of the different components for engineering applications. TiN, CrN, AlTiN
22
23 and different multilayer coatings are commercially available under different trade names. Apart
24
25 from these nitride coatings, another method of enhancing the surface properties is to treat the
26
27 engineering component under nitrogen plasma. Generally nitridation under definite surface bias
28
29 potential penetrate the surface upto a certain depth (depending on the applied voltage and plasma
30
31 treatment time) and thereby increase the surface hardness and corrosion resistance property of
32
33 the metal component under engineering applications (Mukherjee et al 2004, Rao et al 2005).
34
35 Carburisation is also a standard method of surface hardening. It is a heat treatment process in
36
37 which iron or steel is heated in the presence of another material (in the range of 900 to 950 °C)
38
39 which liberates carbon as it decomposes. Depending on the amount of time and temperature,
40
41 varying amount of carbon diffuses into the part and the outer surface becomes hard via the
42
43 transformation from austenite to martensite during quenching, while the core remains soft and
44
45 tough as a ferritic and/or pearlite microstructure. Now other than these conventional methods of
46
47 surface engineering (by nitridation or carburisation) another class is carbon based coating
48
49 material popularly termed as Diamond like Carbon (DLC) coatings which have been in use for
50
51 decades. But the main drawback of this type of coating is incompatibility with steel and other
52
53
54
55
56
57
58
59
60
61
62
63
64
65

1
2
3
4 metals which has carbon solubility in the structure. There is a need of interlayer of chromium or
5
6 titanium nitride before depositing DLC layer to prevent carbon diffusion into the substrate
7
8 structure. Moreover the tribological performance of DLC reduces due to inherent stress inside
9
10 the structure in the order of GPa. An unique class of material has been found which can be
11
12 deposited over any substrate material with good tribological performance. This material is an
13
14 interpenetrating network of amorphous hydrogenated carbon and quartz like oxygenated silicon
15
16 and is called diamond-like-nanocomposite (DLN). Due to the presence of silicon in the structure,
17
18 the adhesion to different substrates increases and internal stress reduction occurs.
19
20
21
22
23

24 DLN coatings have been in use since early 1990s. V. F. Dorfman first reported synthesis of such
25
26 unique class of material (Dorfman 1992). Later on Bekaert Advanced Coating Technologies
27
28 (formerly known as Advanced Refractories Technologies) and Russian and American scientists
29
30 patented DLN coatings for various protective coatings applications (Dorfman et al 1994,
31
32 Dorfman et al 1995, Cooper et al 2007, Emerson et al 1996, Dorfman et al 1998, Bosley et al
33
34 1998, Hooshang 2000, Neernick et al 2001, Neernick et al 2001, Jacquet et al 2006. DLN
35
36 coatings also have been used in micro-electromechanical systems (MEMS) applications like
37
38 LIGA (German acronym for Lithographie, Galvanoformung und Abformung) structures (Prasad
39
40 et al 2003). Bekaert Advanced Coating Technologies, Belgium have used plasma enhanced
41
42 chemical vapor deposition (PECVD) method for growing such composite films. Chinese
43
44 researchers have successfully used ion beam technology for growing DLN films (Ding et al
45
46 1999). South Korean researchers have reported thermally activated CVD process for growth of
47
48 DLN films (Yang et al 2000). Moreover Diamond-like carbon/nanosilica composite films have
49
50 been deposited on silicon substrates, making use of the electrolysis of methanol–
51
52 dimethylethoxydisilane (DDS) solution at low temperature (Yan et al 2004). In the present work
53
54
55
56
57
58
59
60
61
62
63
64
65

1
2
3
4 we have used PECVD with similar reactor used by Bekaert Advanced Coatings Technology,
5
6 Belgium. The reactor was available with one of our research collaborator Meghnad Saha Institute
7
8 of technology, Techno India Group.
9

10
11 DLN have been characterized by various researchers (Yang et al 2003, Yang et al 2003,
12
13 Venkatraman et al 1999, Neernick et al 1998, Bozhko et al 1998, Kester et al 1999, Dorfman
14
15 1998, Polyakov et al 1997, Scharf et al 2007, Narayan 2005, Bursikova et al 2007, Pandit et al
16
17 2003, Venkatraman et al 1997, Neernick et al 1998, Scharf et al 2003, Hauert et al 2003,
18
19 Maalouf et al 2006, Pollak et al 1997, Platon et al 2001, Sheeja et al 2005, Kobayashi et al 2006,
20
21 Logothetidis 2007). They have unique bulk and surface properties including excellent thermal
22
23 stability (Yang et al 2003). The applications of DLN films include tribological coatings,
24
25 chemical protective coatings (Venkatraman et al 1999, Neernick et al 1998, Kester et al 1999,
26
27 Scharf et al 2007, Neernick et al 1998, Scharf et al 2003) and abrasion-resistant coatings for IR
28
29 windows. They have unique control over optical properties and electrical properties (Bozhko et
30
31 al 1998, Dorfman 1998, Polyakov et al 1997). Moreover it finds indirect application in the field
32
33 of biomedical implants. Hydroxyapatite is widely used plasma sprayed coating for
34
35 oseointegration of implants. DLN films have been reported to improve the adhesion of these
36
37 coatings to the substrates (Narayan 2005). It has excellent adhesion (Pandit et al 2003) to a
38
39 variety of substrate materials due to a low residual stress, Moreover these films have found
40
41 application as biosensors (Maalouf et al 2006). DLC coatings have been tried as protective wear
42
43 resistant coating in joint prostheses (Platon et al 2001, Sheeja et al 2005). Diamond-like carbon
44
45 (DLC) films were deposited onto UHMWPE and PMMA substrates using plasma CVD process
46
47 (Kobayashi et al 2006). To improve adhesion of DLC films, substrates were plasma treated
48
49 before DLC deposition. Carbon based films have found to be haemobiocompatible as well
50
51
52
53
54
55
56
57
58
59
60
61
62
63
64
65

1
2
3
4 (Logothetidis 2007). But so far there are not many literatures about DLN films in biomedical
5
6 applications. Researchers at Department of Cardiology, University Hospitals Leuven, Belgium
7
8 (Scheerder et al 2000) have used either DLN (or Dylun, Bekaert, Kortrijk, Belgium) coated or
9
10 non-coated stents, randomly implanted in two coronary arteries of 20 pigs. The results indicate
11
12 that the diamond-like nanocomposite stent coatings are compatible, resulting in decreased
13
14 thrombogenicity and decreased neointimal hyperplasia. DLN coating may have been in use
15
16 commercially worldwide with different trade names, but there is no reported data available about
17
18 its use in orthopedic applications. DLN films represent a significant advance over conventional
19
20 diamond-like films in both stability and ability to tailor specific properties over a wide range.
21
22 The properties are summarized in the table 1 and compared with diamond and DLC coatings.
23
24
25
26
27

28
29 In the present study we have deposited DLN coatings by PECVD method over different
30
31 substrates like, SS 316L, Glass, Si (100), ceramic (Al_2O_3), Ultra High Molecular Weight
32
33 Polyethylene (UHMWPE), CoCr alloy, Ti6Al4V alloy etc. Most of these materials have been in
34
35 use as load bearing orthopedic implants, like hip joint, knee joint etc (Rahaman et al 2007).
36
37 Generation of UHMWPE wear particles is prime concern for failure of such implants. Many
38
39 protective coatings like TiN, CrN (Ionbond® Coatings) or oxidized zirconium (Oxinium, Smith
40
41 & Nephew®) have so far been used to reduce polyethylene wear of implants. But deposition of
42
43 these coating materials involves high temperature processing of implant materials, which
44
45 enhances the chance of losing its mechanical property at high processing temperatures. DLN
46
47 coating has been deposited at as low as 100°C, thereby enabling to coat even polymeric
48
49 materials. So far DLN may have not been used as protective coating for biomedical applications.
50
51
52
53 Although there are reports of DLC being used as protective coating in orthopedic implants
54
55
56
57 (Hauert et al 2003, Platon et al 2001, Sheeja et al 2005, Kobayashi et al 2006, Logothetidis
58
59
60
61
62
63
64
65

1
2
3
4 2007, McNamara et al 2001, A. Grill 2003, R. Hauert 2003). R. Hauert in his review article
5
6 (2003) after describing contradicting results from various literatures has commented that the
7
8 superior tribological properties of DLC in various environments can probably not be easily
9
10 applied for hip joints and other load bearing implants as the build up of a transfer layer does not
11
12 take place, and the UHMWPE counterpart still shows wear. According to Hauert DLC coated
13
14 load bearing implants sliding against DLC coated counterparts or against ceramics may show
15
16 good ‘ceramic like’ tribological properties, but he questioned of any real improvement in wear
17
18 performance against the existing ceramic/ceramic or metal/ceramic bearings. Therefore attempt
19
20 has been made to find an alternative DLN based protective coating, which does not have intrinsic
21
22 stress and do not require interlayer to prevent carbon dissolution. Diamond like nanocomposite
23
24 coating is expected to enhance the tribological performance of orthopedic implants. Moreover
25
26 DLN has been proven to be non-toxic. We hope that DLN coating would be suitable material for
27
28 biomedical tribology. The coating has been characterized by Raman Spectroscopy, Fourier
29
30 Transform Infrared Spectroscopy (FT-IR), Transmission Electron Microscopy (TEM), X-ray
31
32 Diffraction (XRD) for structural evaluation and mechanical properties like hardness and young’s
33
34 modulus have been tested. Thicknesses of the coatings have been calculated by stylus
35
36 profilometer and growth rates were calculated from thickness measurements. Moreover
37
38 tribological behavior has been evaluated by ball-on-disc tribometer.
39
40
41
42
43
44
45
46
47
48
49

50 **2. Materials & Methods:**

51 *2.1 PECVD Reactor*

52
53
54 One plasma enhanced chemical vapor deposition (PECVD) reactor has been used for deposition
55
56 of DLN coatings as depicted in figure 1. This reactor had been in use for commercial production
57
58
59
60
61

1
2
3
4 of Dyllyn® protective coatings. It has a rotating substrate holder at the top, which rotates at 2-3
5
6 rpm speed. There is a liquid precursor feeder at the bottom, through which liquid siloxane enters
7
8 into the vacuum and due to difference in pressure evaporates into vapor form. There is one
9 tungsten filament forming an arc above the liquid precursor feeder. This filament is negatively
10
11 biased and there is electron emission from the filament, which ionizes the precursor vapor. These
12
13 ionized precursor species is attracted by the substrate holder, which is again negatively biased at
14
15 higher voltage. Before starting the precursor flow, argon gas is introduced into the reactor
16
17 chamber to form plasma. Heavy argon ions bombard the substrates and etch it to clean the
18
19 substrates prior to deposition. There are provisions for resistive heating evaporation and
20
21 sputtering of metal atoms for co-deposition inside this reactor. But during these set of
22
23 experiments metal co-deposition has not been done. The whole chamber is water cooled. There is
24
25 provision for substrate holder cooling as well. This is specially required for polymer substrates.
26
27
28
29
30
31
32
33

34
35 Deposition can be described in four steps: a) plasma etching of the substrate by bombardment of
36
37 the substrate by ions of an inert gas such as Ar, b) introducing a liquid organic precursor
38
39 containing the elements C, H, Si, O to be deposited in suitable proportions (remain substantially
40
41 constant during the deposition process), in the vacuum chamber, at a working pressure of
42
43 between 5×10^{-3} and 5×10^{-2} mbar, c) forming a plasma from the introduced precursor by an
44
45 electron assisted DC-discharge using a filament with a filament current of 50-150 A, a negative
46
47 filament bias DC voltage of 50-300 V and with a plasma current between 0.1 and 20 A, d)
48
49 depositing the composition on the substrate, to which a negative DC-bias of 200 to 1200 V is
50
51 applied, in order to attract ions formed in the plasma. Table 2 describes the substrates used
52
53 during experiments and corresponding processing parameters.
54
55
56
57
58
59
60
61
62
63
64
65

1
2
3
4 *2.2 Physical Characterizations*
5
6
7

8 Fourier Transform Infrared Spectroscopy (FTIR) of the deposited films were done using Perkin
9 Elmer Spectrum 100. Scan range was from 4000 – 650 cm⁻¹. Source was MIR and detector was
10 MIR TGS. Beamsplitter used was OptKBr and the instrument resolution was 4.00 cm⁻¹. IR
11 accessory type was Universal ATR and UATR Crystal Combination was Diamond/ZnSe.
12
13
14
15
16
17

18
19 Raman spectroscopy is by far the best non-destructive way to study the bonding structure and
20 quality of the DLN films. The Raman microprobe studies were carried out in Durham University,
21 UK. The Raman spectrometer was based on a commercial Raman microscope (Ramascope 1000,
22 Renishaw) equipped with a 50x ULWD, 0.55 NA objective (Olympus). The DLN films were
23 probed by a diode-pumped solid-state laser (Opus 532, Laser Quantum), which emitted light at
24 the green region of spectrum at 532 nm. The laser (5 mW intensity at source) beam was focussed
25 to about <2 μm diameter spot and spectra were obtained with 5 minute acquisition time.
26
27
28
29
30
31
32
33
34
35
36

37 Transmission electron microscopy (TEM) was done using model Tecnai G² 30 ST of FEI
38 Company, Europe. The X-ray diffraction patterns of the samples were recorded in X'pert Pro
39 MPD diffractometer (PANanalytical) operating at 45 kV and 35 mA using Ni-filtered CuKα
40 radiation. The XRD data were recorded in X'celerator from 10° to 100° with glancing angle thin
41 film attachment. DLN coatings were seen under scanning electron microscope (LEO 430i
42 STEROSCAN, U.K.) for microstructural evaluation of wear track along with EDAX analysis.
43
44
45
46
47
48
49
50
51
52 Roughness was measured by surface profilometer (Surtronic 3p, Form Talysurf Plus, Rank
53 Taylor Hobson Ltd. U.K.). Double sided tape had been used as masking material to form an
54 uncoated portion on the substrate. Scanning of the coating, starting from coated portion to
55 uncoated portion, produces a step in the roughness profile of the substrate. The height of the step
56
57
58
59
60
61
62
63
64
65

1
2
3
4 is the thickness of the coating. If this thickness is divided by the deposition time of the coating,
5
6 we get the growth rate of the plasma enhanced chemical vapor deposition (PECVD).
7
8
9

10 *2.3 Mechanical Characterizations*

11
12
13
14 The micro-hardness on DLN coated steel and glass substrates was measured according to
15
16 standard ASTM E2546 using Nanovea Micro Hardness Tester (MHT) carried out at Micro
17
18 Photonics Inc. The test conditions were as follows: Vickers diamond indenter, Maximum force
19
20 applied was 0.10 N, loading rate was 0.20 N/min and unloading rate was also 0.20 N/min. The
21
22 values were computed using Oliver & Pharr method.
23
24
25
26

27
28 Scratch resistance was measured by using sphero-conical stylus (Nanovea Micro Scratch Tester
29
30 of Micro Photonics Inc.) of 10 micron radius with initial load of 0.045 N and final load of 2.0 N
31
32 at loading rate of 2.0N/min. Scratch length was 3 mm and scratching speed was 3.07mm/min.
33
34
35

36
37 Wear and friction experiments were done on DLN coated substrates with a ball on disc
38
39 arrangement. Radius of the steel ball was 6.35 mm and a constant load of 1 N was applied while
40
41 rotating in a 4 mm diameter circle at constant speed.
42
43
44

45 **3. Results & Discussions**

46 47 48 *3.1 Physical Properties*

49
50
51 Diamond-like-nanocomposite is composite in nature at the molecular level. The chemical
52
53 formulae of the siloxane precursor used for DLN synthesis composed of units of the form R_2SiO ,
54
55 where R is a hydrogen atom or a hydrocarbon group. A siloxane has a branched or unbranched
56
57 backbone of alternating silicon and oxygen atoms -Si-O-Si-O- with side chains R attached to the
58
59
60
61
62
63
64
65

1
2
3
4 silicon atoms. Here we have used triphenyle nona methyle penta siloxane precursor. Liquid
5
6 precursor is bubbled into the vacuum inside the reactor, where it evaporates into vapor form.
7
8 These neutral molecules get ionised by electrons emitted thermoionically from tungsten filament
9
10 and form charged hydrocarbon and SiO species, which are being attracted towards the negatively
11
12 biased substrate holder. The DLN coating thus deposited is amorphous in nature and can be
13
14 described as networks of amorphous hydrogenated carbon and oxygenated silicon entangled
15
16
17
18
19 with each other.
20

21
22 Raman spectra of DLN films deposited on different substrates are shown in figure 2. The broad
23
24 asymmetric bands in the $1000-1700\text{ cm}^{-1}$ are typical characteristics of amorphous carbon or
25
26 diamond-like films (Yang et al 2003). The Raman spectra were curve fitted to obtain a Gaussian
27
28 deconvolution into D and G peaks as shown in the table 3. The G peak is a characteristic of
29
30 single crystalline graphite, which results due to E_{2g} C-C stretching vibrations in the graphite
31
32 layer and the D peak is a characteristic of disordered graphite, which results due to the A_{1g}
33
34 vibrational modes (J. Robertson 2002). Hence D stands for ‘disorder’ and G stands for
35
36 ‘graphite’. In amorphous carbon films, the electronic properties are controlled by the sp^2 sites
37
38 with π bonds, and the mechanical properties and controlled by the sp^3 sites with σ bonds (J.
39
40 Robertson 1994).
41
42
43
44
45

46
47 Therefore the physical properties of the DLN films can be explained by the sp^3/sp^2 ratio, which
48
49 is correlated to the position and intensity ratio (I_D/I_G) of the D and G peaks. The positional shift
50
51 of the Raman D and G peaks can reflect the difference in actual film structures (Yang et al
52
53 2003)**Error! Bookmark not defined.**; however, the peaks can also be a little shifted due to the
54
55 difference in light source of the Raman spectrometer, curve fitting parameters applied and so on.
56
57
58

59 In table 3, the comparison shows that the I_D/I_G ratio in the Raman spectra of the DLN films
60
61

1
2
3
4 coated on different substrates have gradually increased from 1.53 for CrCoMo alloy to 2.71 for
5
6 Ti6Al4V alloy. This increase in I_D/I_G ratio is associated with a relative increase in the sp^3 site
7
8 content (or a relative decrease in the sp^2 site content) in the respective DLN films. It is regarded
9
10 that a higher graphite (or sp^2) content in the amorphous carbon films reduces the hardness of the
11
12 films. Therefore we can predict to observe an increasing order of hardness in the DLN films with
13
14 an increasing value of I_D/I_G ratio.
15
16
17
18

19
20 Figure 3 shows FT-IR spectra of DLN films on stainless steel & glass substrates. Major
21
22 absorption band of the Si-O stretching in the $1100-1000\text{ cm}^{-1}$ range is observed in both the FT-IR
23
24 spectra of DLN films. Second prominent absorption band we could find in the $3100-2800\text{ cm}^{-1}$
25
26 range was of the C-H stretching. The C-H absorption band in the $3100-2800\text{ cm}^{-1}$ range is typical
27
28 for sp^3 - and sp^2 -bonded carbon. These C-H and Si-O stretching peaks prove that the DLN films
29
30 mainly consist of hydrogenated carbon (C:H) and oxygenated silicon (Si:O) networks. Apart
31
32 from the interpenetrating networks of Si:O and C:H, there are also the presence of non-graphitic
33
34 carbon and Si-C like bondings. There is a small hump of Si-C stretching in the 800 cm^{-1} region.
35
36 Presence of non-graphitic bonding of carbon is confirmed by C=C stretching peaks appearing in
37
38 the 1580 cm^{-1} region. Also we could see Si-H stretching appearing in 2100 cm^{-1} region. Our
39
40 results exactly match with reported literature values (Yang et al 2003). Chemical composition
41
42 was also studied using EDAX of the worn films.
43
44
45
46
47
48

49
50 Figure 4 indicates that XRD could not detect any crystallinity within its resolution. XRD patterns
51
52 were taken from DLN coatings on glass substrates. The hump around $2\theta = 26.5^\circ$ in the scan is
53
54 typical for amorphous films grown on quartz microscope slides, due to the presence of SiO_2 in
55
56 the bottom glassy substrate. To further prove the amorphous nature of the film, transmission
57
58 electron microscopy was done of DLN coatings. DLN deposited onto 50 micron thick aluminium
59
60
61
62
63
64
65

1
2
3
4 foil has been plasma etched from the opposite uncoated side of the foil, so as not to damage the
5
6 DLN coating. Once one hole has been created in the foil, DLN film was seen in and around the
7
8 created hole under transmission electron microscope. Figure 5 shows typical TEM micrographs,
9
10 which are characteristics of amorphous structure (Yang et al 2003).
11
12
13

14
15 The average Ra roughness of the bare steel substrates before deposition was found to be 0.1
16
17 micron. DLN coatings follow the contours of the underlying substrate. The Ra roughness does
18
19 not vary much after deposition. It is found to be 0.15 micron. Roughness of DLN films deposited
20
21 on laboratory glass slide substrates was beyond instrument range as it followed the very smooth
22
23 surface of glass slides. The advantage of this is that there is no need of post-deposition polishing
24
25 of DLN coating on well polished substrates. Any other wear resistance protective coating has to
26
27 be polished to reduce the surface roughness prior to application. Upper scan profile of Figure 6
28
29 shows a 1.75 micron step in the profilometer scan of the substrate for DLN on SS 316 L
30
31 combination. The coating had been grown for 100 minutes, thus the growth rate can be
32
33 calculated to be 1.04 $\mu\text{m/hr}$. Bottom scan profile of figure 6 shows one trough in the scan profile
34
35 of DLN on glass slide, as the stylus moves from coated portion through uncoated portion to other
36
37 side of the coated portion of the substrate. The thickness was found to be 660 nm. Deposition
38
39 time was 29 minutes (table 2). So the growth rate can be calculated to be 1.365 $\mu\text{m/hr}$. It has
40
41 been found that typical growth rate varies between 1 – 3 $\mu\text{m/hr}$.
42
43
44
45
46
47
48
49

50 *3.2 Mechanical Properties & Tribology*

51
52

53 Mechanical properties alongwith roughness values of DLN coatings on steel and glass substrates
54
55 have been tabulated in table 4. Indentation with 0.1N load was not clearly visible, so tests were
56
57 performed with 1N & 3N loads. Figure 7a shows micro-indentation mark on DLN coating. It is
58
59
60
61
62
63
64
65

1
2
3
4 found that DLN deposited on stainless steel has higher hardness value of 17 GPa in comparison
5
6 to hardness value of 14 GPa of DLN coatings deposited on glass substrates. Not only the
7
8 hardness values are higher for steel substrates but also Young's Modulus for steel substrates is
9
10 132 GPa in compare to 73 GPa for glass substrates. The literature values of hardness for this
11
12 class of materials vary between 12-17 GPa (Bozhko et al 1998), which is in complete agreement
13
14 with present findings. Now, whereas plasma immersion ion implantation (PIII) techniques could
15
16 give only 8-9 GPa of surface hardness of AISI 304L stainless steel (Rao et al 2005).
17
18
19
20
21

22 Scratch resistance has been reported by critical force L_C at which damage of the coating occurs.
23
24 The critical load is optically defined by the point where the substrate is completely uncovered in
25
26 the scratch track for a length equal or greater than the scratch width. The optical micrograph in
27
28 figure 7b shows typical scratch track. At least five measurements were done on each sample to
29
30 calculate the average L_C . The critical load L_C for DLN coatings on steel substrates was found to
31
32 be 0.618 N and the L_C for DLN coatings on glass substrates was found to be 0.196 N. With such
33
34 good adhesive strength and hardness values, DLN could find wide application as wear resistant
35
36 coating.
37
38
39
40
41

42 Sliding wear behavior of steel ball sliding against DLN coating under dry condition is shown in
43
44 table 5. The experiments were conducted under room temperature conditions. Steel ball was
45
46 made to revolve in 4 mm diameter circle on DLN coated substrates. The steady state coefficient
47
48 of friction (COF) changes from 0.043 to 0.092 when revolution changes from 90000 to 110000.
49
50 The corresponding calculated wear factors are $1.26 \times 10^{-7} \text{ mm}^3/\text{N-m}$ and $1.33 \times 10^{-7} \text{ mm}^3/\text{N-m}$
51
52 respectively. Obviously the wear volume will increase if the ball is made to revolve for higher
53
54 number of revolutions of 150000, but in that case the average COF strikingly increases to 0.143,
55
56 much higher than 90000 and 110000 revolutions. Whereas the reported literature COF values for
57
58
59
60
61
62
63
64
65

1
2
3
4 such wear experiments have always been below 0.1 (Neernick et al 1998, Neernick et al 1998).
5
6 This anomaly in COF values between reported and available literature may be due to the fact
7
8 that, as the ball is made to slide for longer duration, the underneath substrate comes out due to
9
10 wearing of DLN coating and thus the resultant values of friction correspond to the values
11
12 between steel ball sliding against bare Si substrate. This is evident from the SEM images of
13
14 figure 8, where bare Silicon substrate is visible due to wearing out of DLN coating. Moreover the
15
16 EDAX from whitish portion of the wear groove indicates presence of Fe, Co, Ni, and O which is
17
18 typical of the steel ball composition. Thus there is clear evidence of material transfer between
19
20 ball and coated substrate. Figure 9 shows the profilometer scan of the wear groove. The depth of
21
22 the groove shows 1.5 micron and whereas the coating thickness was less than one micron. This
23
24 difference between coating thickness and wear track depth further confirms exposure of the
25
26 underneath silicon substrate.
27
28
29
30
31
32

33 34 **4. Conclusions**

35 36 37 *4.1 PECVD*

- 38
39
40
41 1. DLN has been successfully deposited on many types of substrates, including polymers,
42
43 glass, ceramics & metals (including aluminum, stainless steel, silicon) by PECVD.
44
45
- 46
47 2. There was no need for interlayer prior to DLN deposition on all the substrates.
48
49
- 50
51 3. Large area deposition ($\sim 3000 \text{ cm}^2$) has been achieved in the PECVD reactor.
52

53 54 *4.2 DLN Coating*

- 55
56
57 1. DLN films mainly consist of hydrogenated carbon (C:H) and oxygenated silicon (Si:O)
58
59 networks, as evident from FT-IR spectra.
60
61

2. Presence of sp^3 carbon and sp^2 graphite inside the structure is evident from Raman Spectroscopy.
3. Films are not only x-ray amorphous but also it is nanocomposite in nature under TEM micrograph.

4.3 Mechanical Properties

1. DLN coatings follow the contours of the underlying substrate with the advantage of non-requirement of post-deposition polishing of well polished parts.
2. Substantial enhancement of the surface hardness is achieved with DLN coating.
3. Adhesion strength is better with metallic substrates than glass substrate which is essential for adhesive wear applications like hip joints and knee joints.
4. After depositing over different materials of biomedical importance, we have successfully deposited DLN coating on femoral components of CoCr alloy based knee implants of complex shape as shown in figure 10. With such good mechanical performance DLN is a potential coating for biomedical tribology.

Acknowledgements

We express our sincere gratitude to Dr. K. H. Sancheti for allowing us to coat indigenously developed “Indus Knee” orthopedic implant. Authors thank Dr. D. Dasu, Head, Bioceramics and Coatings Division to allow us to conduct the above research. Dr. Raghu Bhattacharyya helped in solving many technical problems through discussions. Soumya Sarkar has done the profilometer measurements. Dr. Sandip Bysakh kindly did the TEM measurements. Authors also thank Dr. (Mrs) S. Sen and Mrs S. Roy for their help in taking SEM micrographs. We are thankful to Dr. S.

1
2
3
4 Majumdar for allowing us to do XRD measurements. Mr. Guillaume Begin of Micro Photonics
5
6 Inc. and Mr. Rajkishore Sahani of Material Testing & Metallurgy Group, Aimil Ltd. Kolkata
7
8 have done hardness and scratch resistance testing of DLN coatings. We are grateful to Prof.
9
10 Colin Bain for allowing us to use Raman facility.
11
12
13

14 **References:**

15
16
17
18 Bosley Robert W, Miller Ronald F 1998 October United States Patent 5827040
19
20

21
22 Bozhko A, Chudinov S M, Evangelisti M, Stizza S, Dorfman V F 1998 Materials Science and
23
24 Engineering **C5** 265
25
26

27
28 Bursikova Vilma, Rehulkab Pavel, Chmelikb Josef, Albertia Milan, Spaltc Zbynek, Jancaa Jan,
29
30 Havel Jose 2007 Journal of Physics and Chemistry of Solids **68** 701
31
32

33
34 Cooper Clark V, Tredway William K, Guile Roy N, Rhemer Chris C, Minick Alan B, Chapman
35
36 Leonard W 2007 November Cryogenic bearings, United States Patent 7296965
37
38

39
40 D J Kester A, Brodbeck C L, I L Singer, Kyriakopoulos A 1999 Surface and Coatings
41
42 Technology **113** 268
43
44

45
46 De Scheerder I, Szilard M, Yanming H, Ping X B, Verbeken E, Neerinck D, Demeyere E,
47
48 Coppens W, Van de Werf F 2000 J Invasive Cardiol **12** 389
49
50

51
52 Ding Xing-zhao, Zhang Fu-min, Liu Xiang-Huai, Wang P W, Durrer W G, Cheung W Y, Wang
53
54 S P, Wilson I H; 1999 Thin Solid Films **346** 82
55
56

57
58 Dorfman B F 1998 Thin Solid Films **330** 76
59
60

61
62 Dorfman V F 1992 Thin Solid Films **212:1/2** 267
63
64
65

1
2
3
4 Dorfman Veniamin F, Goel A 1998, March United States Patent 5728465
5
6
7 Dorfman Veniamin F, Pypkin Boris 1994 October United States Patent 5352493
8
9
10 Dorfman Veniamin F, Pypkin Boris 1995 November United States Patent 5466431
11
12
13
14 Emerson Terence P, Gu Alston L 1996 June United States Patent 5529464
15
16
17 F Platon, P Fournier, S Rouxel 2001 Wear **250** 227
18
19
20
21 Fred H Pollak, Benjamin Dorfman 1997 Thin Solid Films **292** 173
22
23
24 Grill A 2003 Diamond and Related Materials **12** 166
25
26
27 Hauert R, Muller U 2003 Diamond and Related Materials **12** 171
28
29
30
31 Hauert R 2003 Diamond and Related Materials **12** 583
32
33
34 Heshmat Hooshang 2000 December United States Patent 6158893
35
36
37 Jacquet J M, Wietig F G, 2006 30 November Patent number: WO 2006/125683
38
39
40 Kobayashi S, Ozeki K, Hirakuri K K, and Aoki H, 2006 Key Engineering Materials **309-311**
41
42
43 1289
44
45
46 Logothetidis 2007 Diamond & Related Materials **16** 1847
47
48
49
50 Maalouf R, Jaffrezic-Renault N, Vittori O, Sigaud M, Saikali Y, Chebib H, Loir A S, Garrelie F,
51
52 Donnet C, Takeno T, Takagi T 2006 Journal of Advanced Science **18** 31
53
54
55
56 McNamara B P, Murphy H, and Morshed M M 2001 Diamond and Related Materials **10** 1098
57
58
59
60
61
62
63
64
65

1
2
3
4 Mukherjee S, Raole P M, Kumar A, Chattoraj I, Rao K R M, Manna I 2004 Surface & Coatings
5
6 Technology **186** 282
7
8
9
10 Neerinck D, Persoone P, Sercu M, Goel A, Kester D, Bray D 1998 Diamond and Related
11
12 Materials **7** 468
13
14
15 Neerinck D, Persoone P, Sercu M, Goel A, Venkatraman C, Kester D, Halter C, Swab P, Bray D
16
17 1998 Thin Solid Films **317** 402
18
19
20
21 Neerinck Dominique, Goel Arvind 2001 March United States Patent 6200675
22
23
24 Neerinck Dominique. Persoone Peter 2001 May United States Patent 6228471
25
26
27
28 Pandit A, Pature N P 2003 J Mat Sc Lett. **22** 1261
29
30
31 Polyakov V I Rukovishnikov A I, Perov P I, Khomich A V, Sukhanov A A, Dorfman B F,
32
33 Pypkin B N, Abraizov M G, Druz B 1997 Thin Solid Films **292** 91
34
35
36
37 Prasad S V, Christenson T R, Dugger M T, Michael J R, and Vanecek C W 2003 American
38
39 Society for Precision Engineering, Winter Topical Meeting - Volume 28
40
41
42
43 Rahaman M N, Yao A, Bal B S, Garino J P, Ries M D 2007 J. Am. Ceram. Soc., **90** 1965
44
45
46 Rao K. Ram Mohan, Mukherjee S, Raole P M, Manna I, 2005 Surface & Coatings Technology
47
48 **200** 2049
49
50
51
52 Robertson J 1994 Pure Appl. Chem. **66** 1789
53
54
55 Robertson J 2002 Materials Science and Engineering R, **37** 129
56
57
58
59 Roger J Narayan 2005 Materials Science and Engineering: C **25** 398
60
61
62
63
64
65

1
2
3
4 Scharf T W and Singer I L 2003 Tribology Letters, **14** 3
5

6
7 Scharf T W, Ohlhausen J A, Tallant D R and Prasad S V 2007 J. Appl. Phys. **101** 0635211
8
9

10 Sheeja D, Tay B K, Nung L N 2005 Surface & Coatings Technology **190** 231
11
12

13
14 Venkatraman C, Brodbeck C, Lei R 1999 Surface and Coatings Technology **115** 215
15
16

17 Venkatraman C, Goel A, Lei R, Kester D, Outten C 1997 Thin Solid Films **308–309** 173
18
19

20 Yan Xing-bin, Xu Tao, Chen Gang , Xue Qun-ji, Yang Sheng-rong 2004 Electrochemistry
21
22 Communications **6** 1159
23
24

25
26 Yang Won Jae, Auh Keun Ho, Li C, Niihara K 2000 J Mat. Sc. Lett. **19** 1649
27
28

29
30 Yang Won Jae, Choab Yong-Ho, Sekinoc Tohru, Shima Kwang Bo, Niiharac Koichi, Auha
31
32 Keun Ho 2003 Materials Letters **57** 3305
33
34

35
36 Yang Won Jae, Choab Yong-Ho, Sekinoc Tohru, Shima Kwang Bo, Niiharac Koichi, Auha
37
38 Keun Ho 2003 Thin Solid Films **434** 49
39
40

LIST OF FIGURE CAPTIONS

Figure 1. Schematic of the PECVD reactor

Figure 2. Raman spectra from DLN films coated on four different substrates: CrCoMo alloy, Si(100) wafer, SS 316L, Ti6Al4V alloy; (532 nm laser, 5mW power, 5 mins. Acquisition)

Figure 3. FT-IR spectra of DLN films deposited on SS 316L and Glass substrates.

Figure 4. XRD micrograph of DLN deposited on glass showing amorphous nature of the deposited film

Figure 5. TEM micrograph around plasma etched hole

Figure 6. Typical Profilometer Scan of the DLN coating for thickness measurement, a) SS 316 L substrate, b) Glass substrate

Figure 7. Optical micrographs of a) microindentation mark on DLN coated glass substrate; b) scratch resistance test mark on DLN coated glass sample

Figure 8. Portion of Wear track of DLN film with EDAX analysis from wear groove and unworn surface.

Figure 9. Profilometer scan across the wear track

Figure 10. Femoral components of Knee Implant, a) Uncoated Co-Cr based alloy, b) DLN Coated

LIST OF TABLE CAPTIONS

Table 1. Comparison of properties among diamond, diamond like carbon (DLC) and diamond like nanocomposite (DLN) coatings.

Table 2. PECVD Deposition conditions

Table 3: Gaussian analyses of Raman spectra deconvoluted into D and G peaks in DLN films coated in different substrates (ν : position, Γ : Full Width at Half Maxima, I : Integrated intensity)

Table 4. Mechanical Properties of DLN coatings

Table 5. Wear and Friction data of steel ball sliding against DLN coated silicon substrate

Figure 1
[Click here to download high resolution image](#)

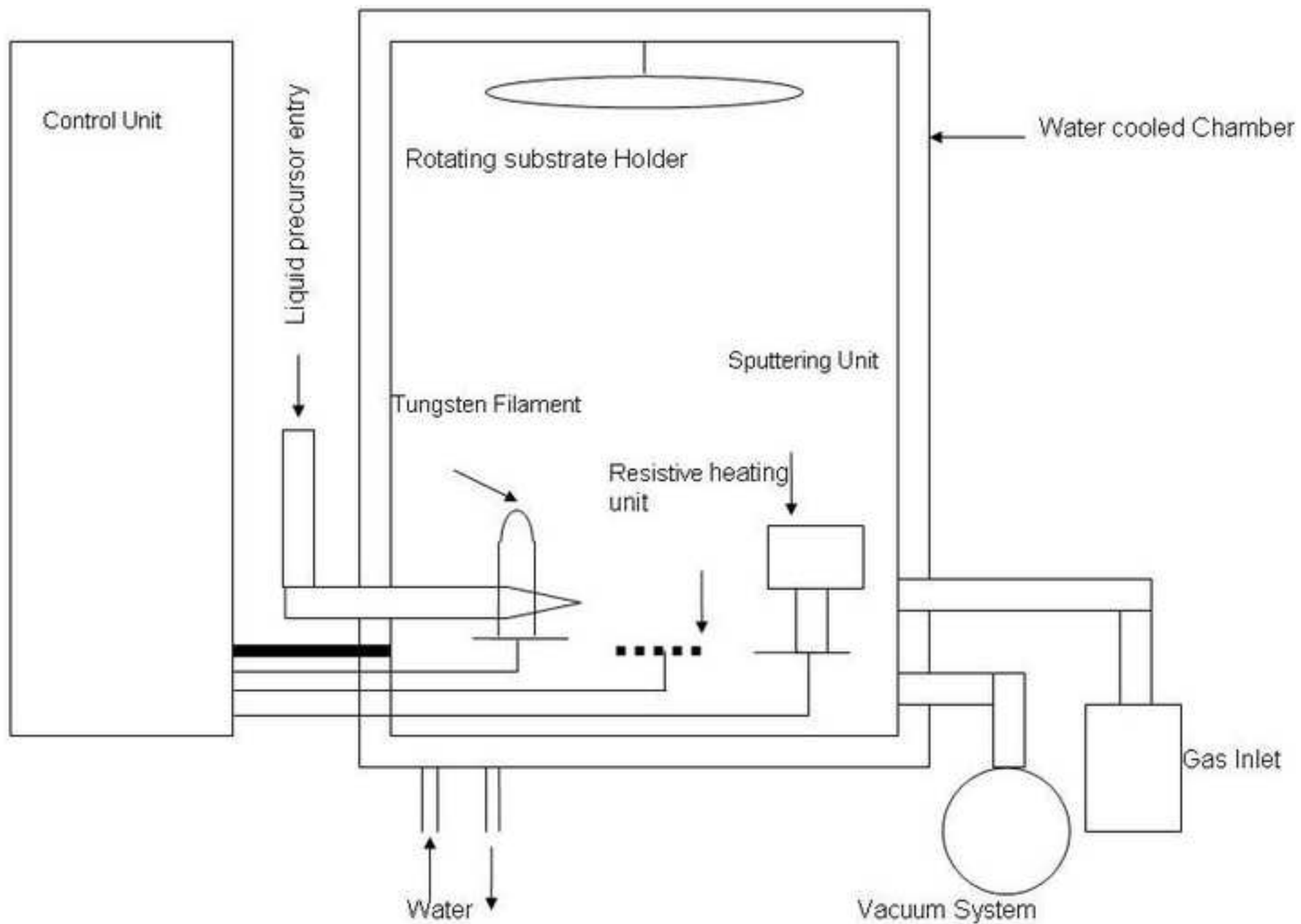


Figure 2
[Click here to download high resolution image](#)

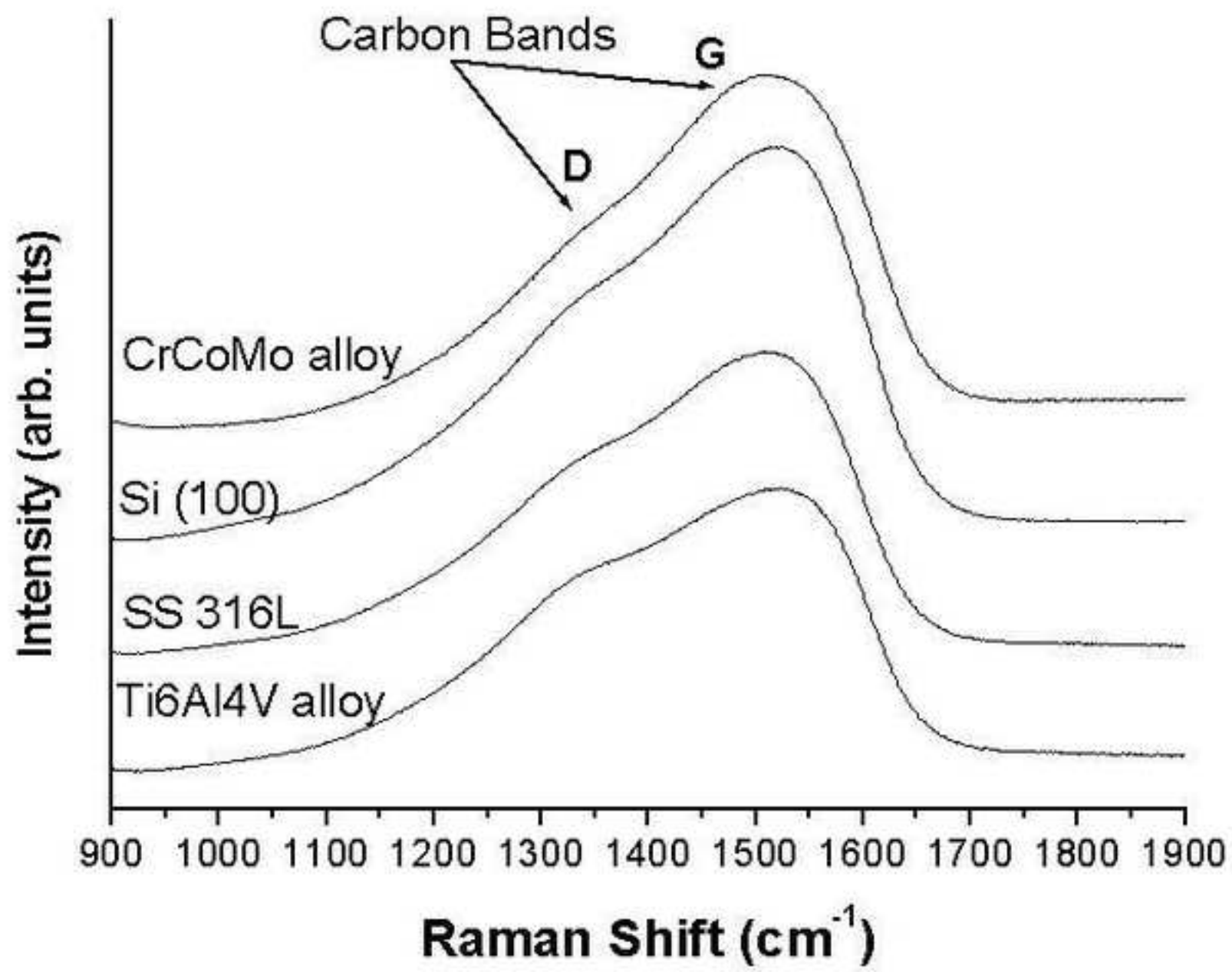


Figure 3
[Click here to download high resolution image](#)

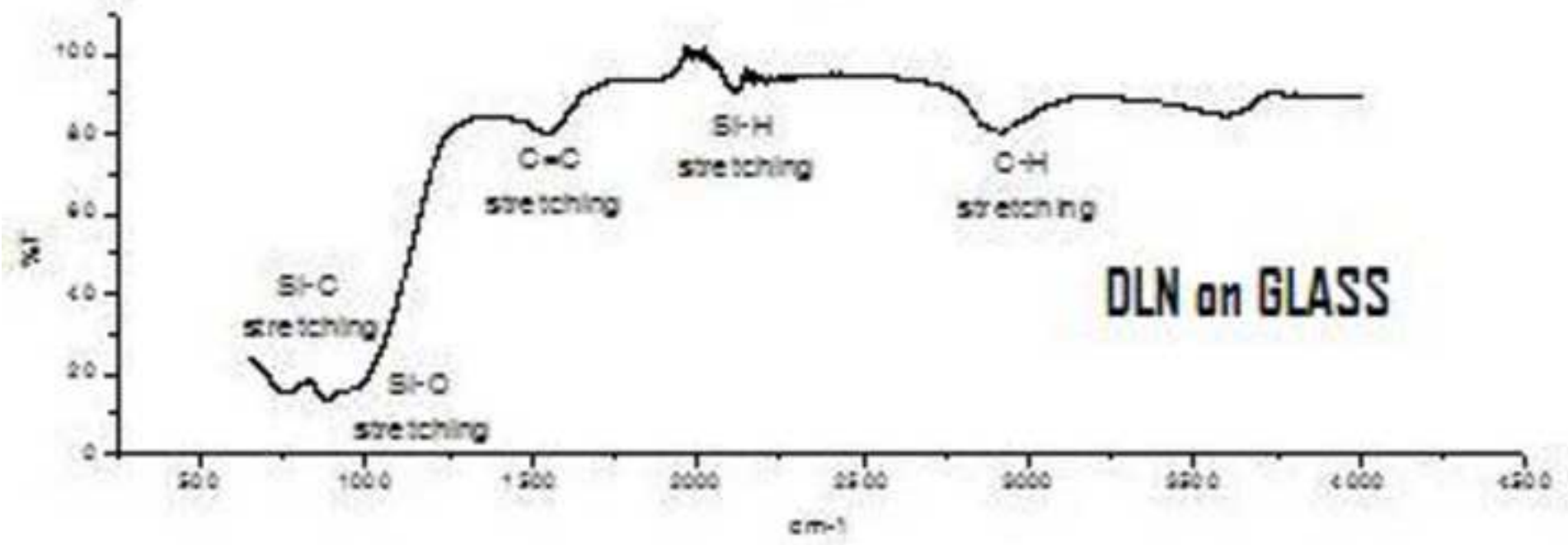
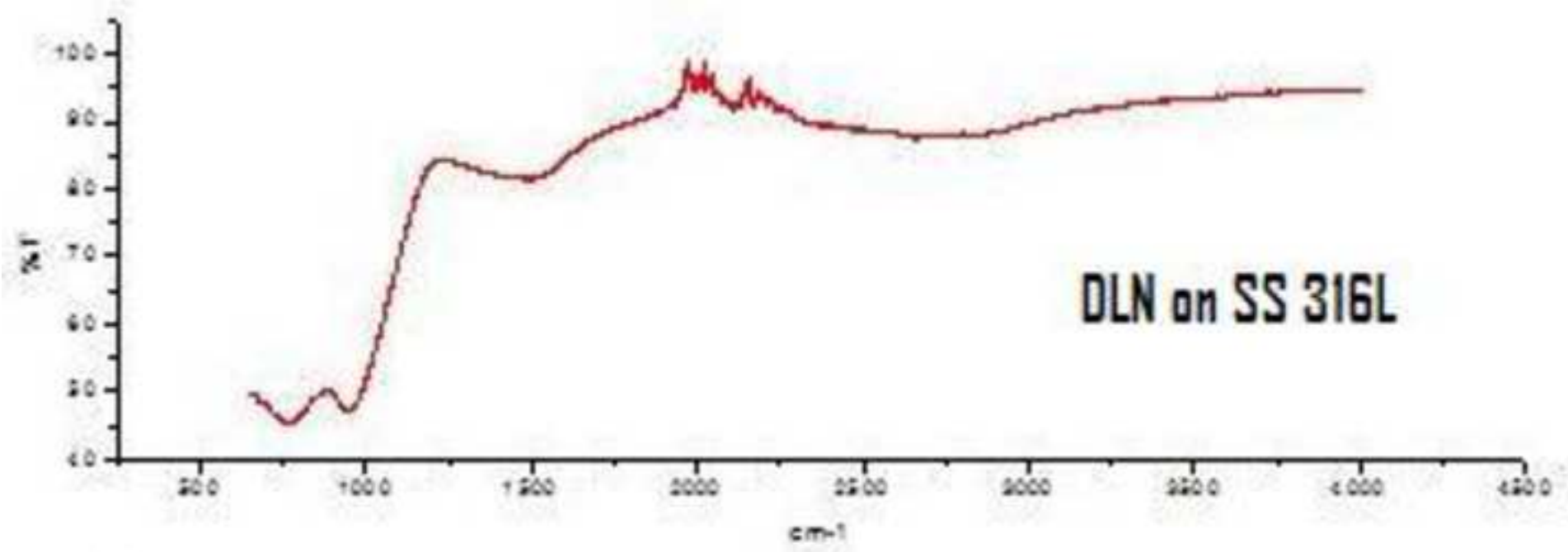


Figure 4
[Click here to download high resolution image](#)

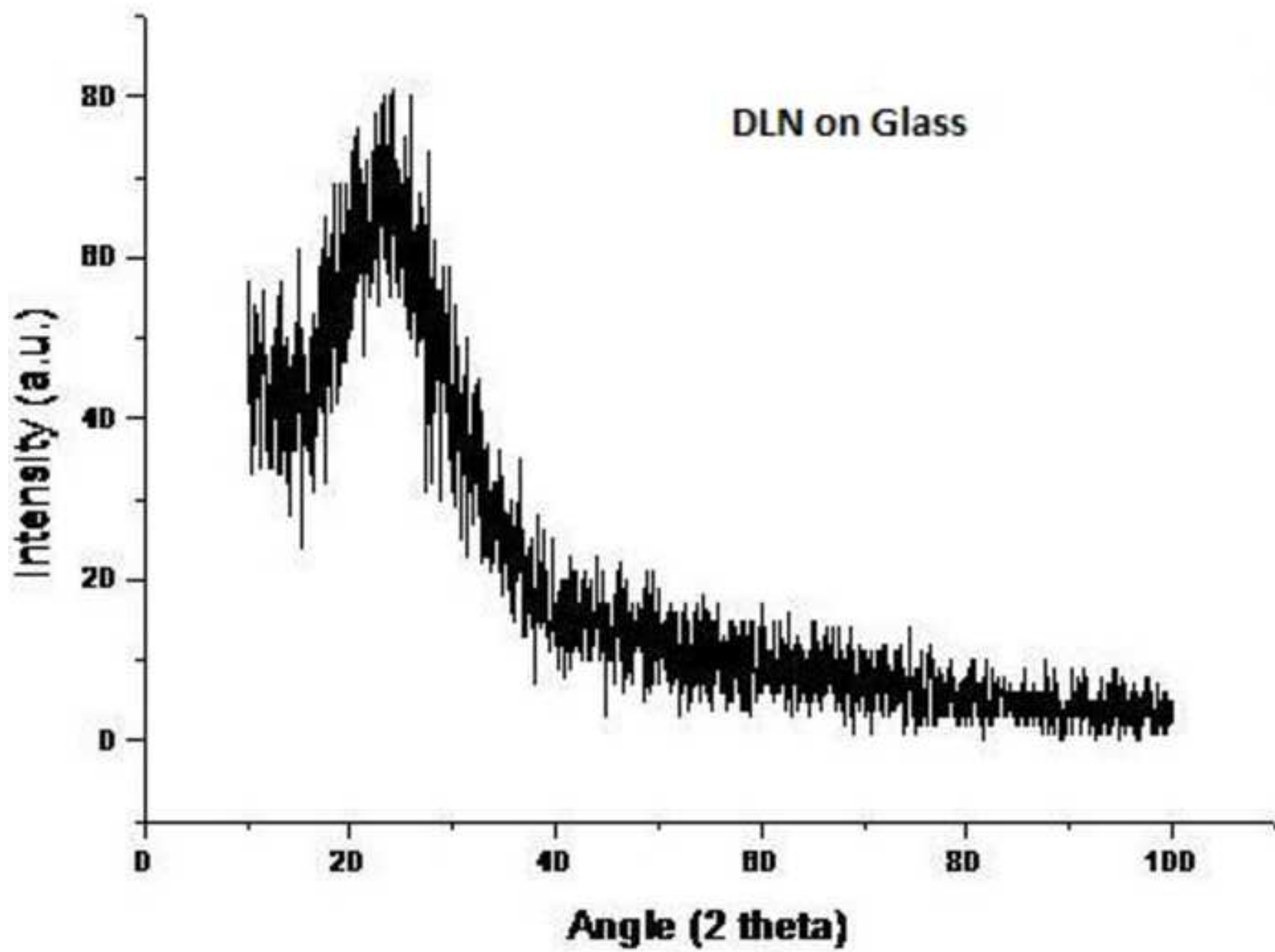


Figure 5

[Click here to download high resolution image](#)

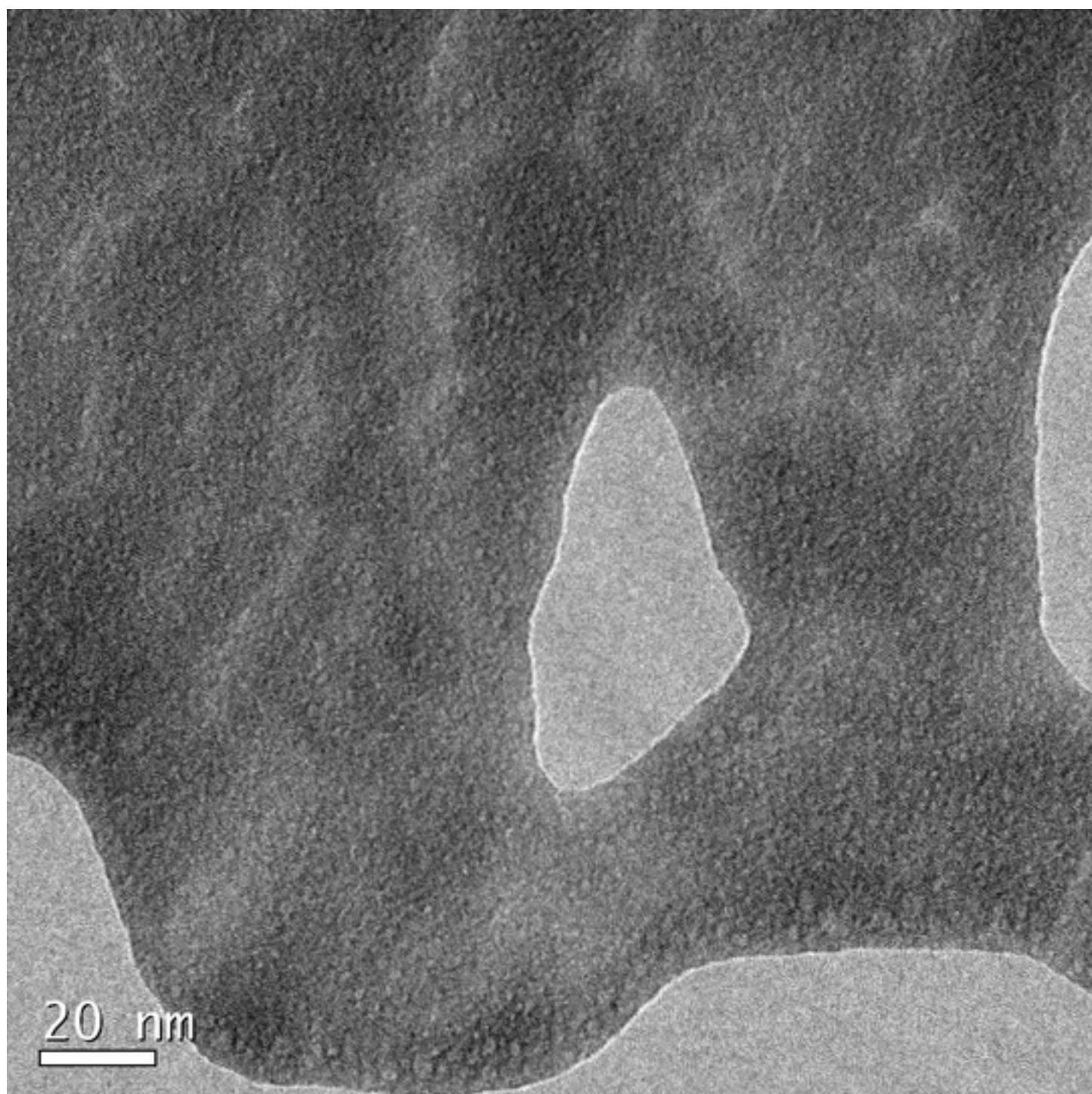


Figure 6
[Click here to download high resolution image](#)

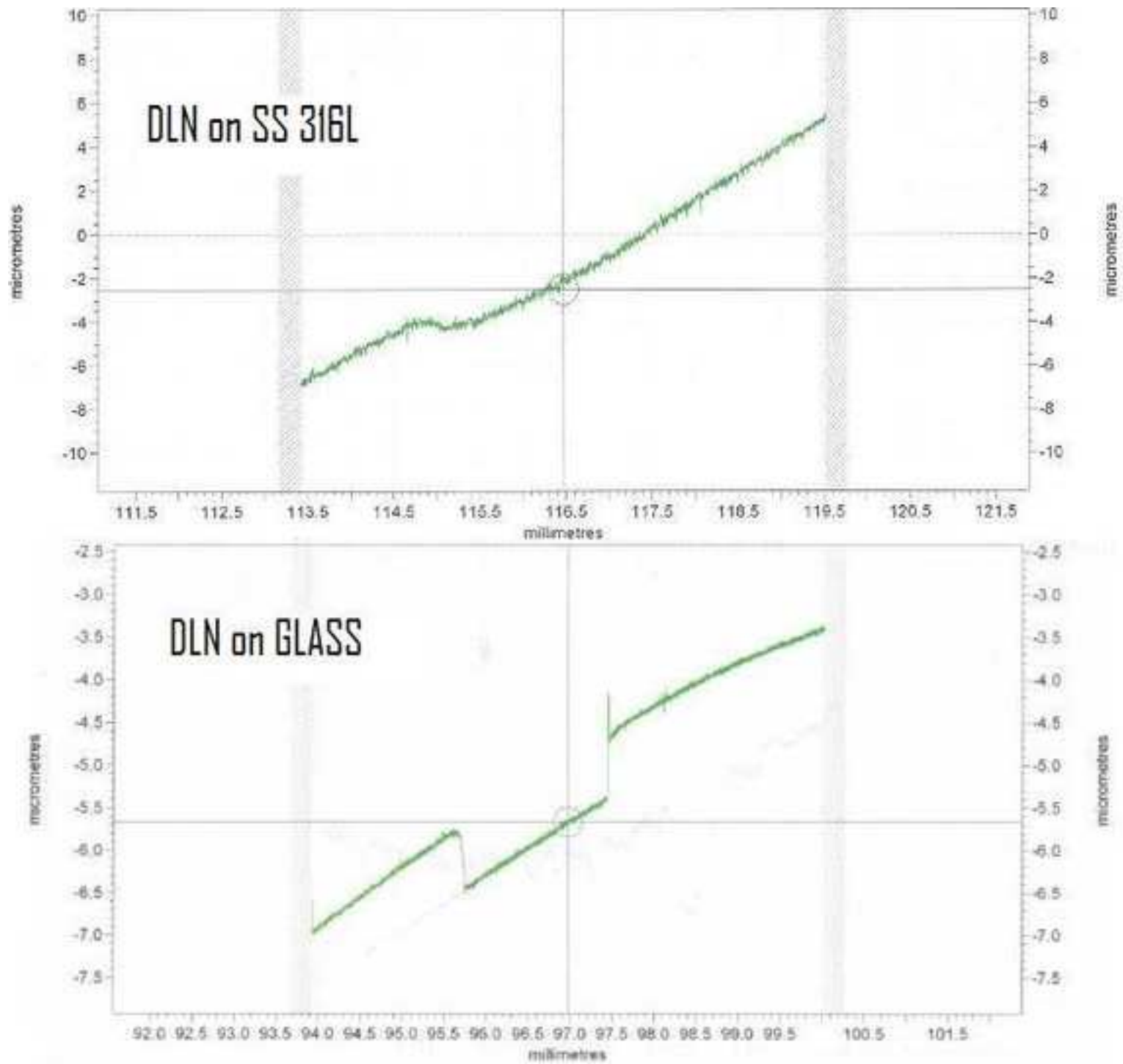


Figure 7

[Click here to download high resolution image](#)

FIGURE A Micrograph of indentations – GL 092 – 1N
500x magnification (image width 0.0625mm)

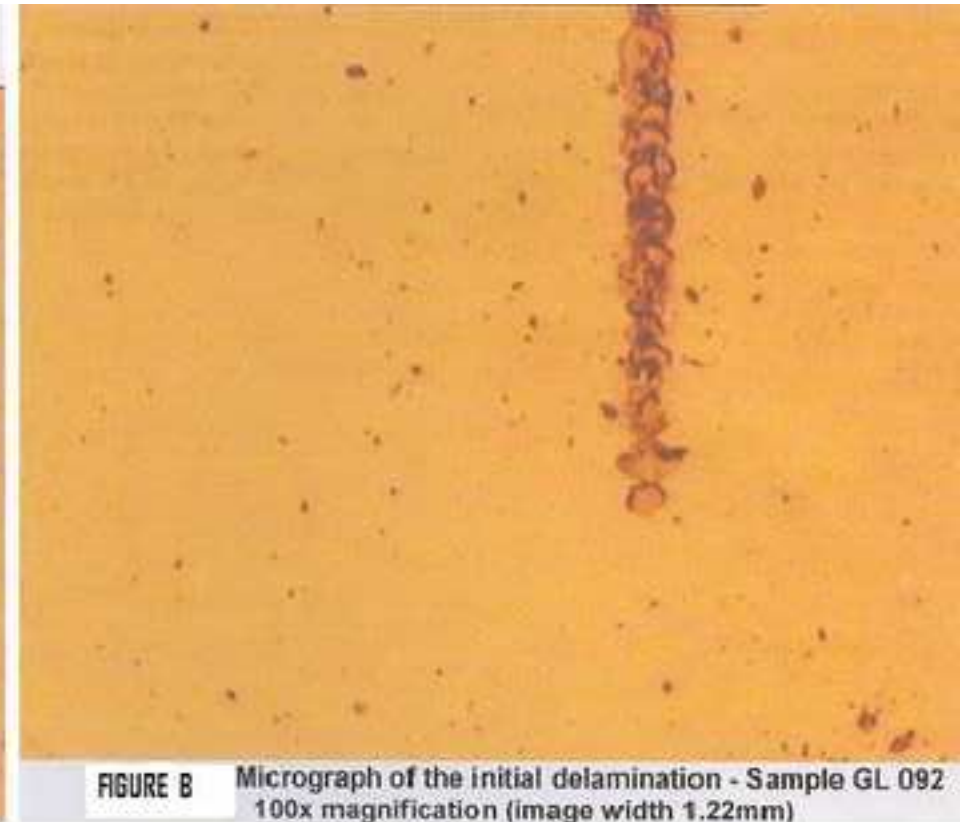


FIGURE B Micrograph of the initial delamination - Sample GL 092
100x magnification (image width 1.22mm)

Figure 8
[Click here to download high resolution image](#)

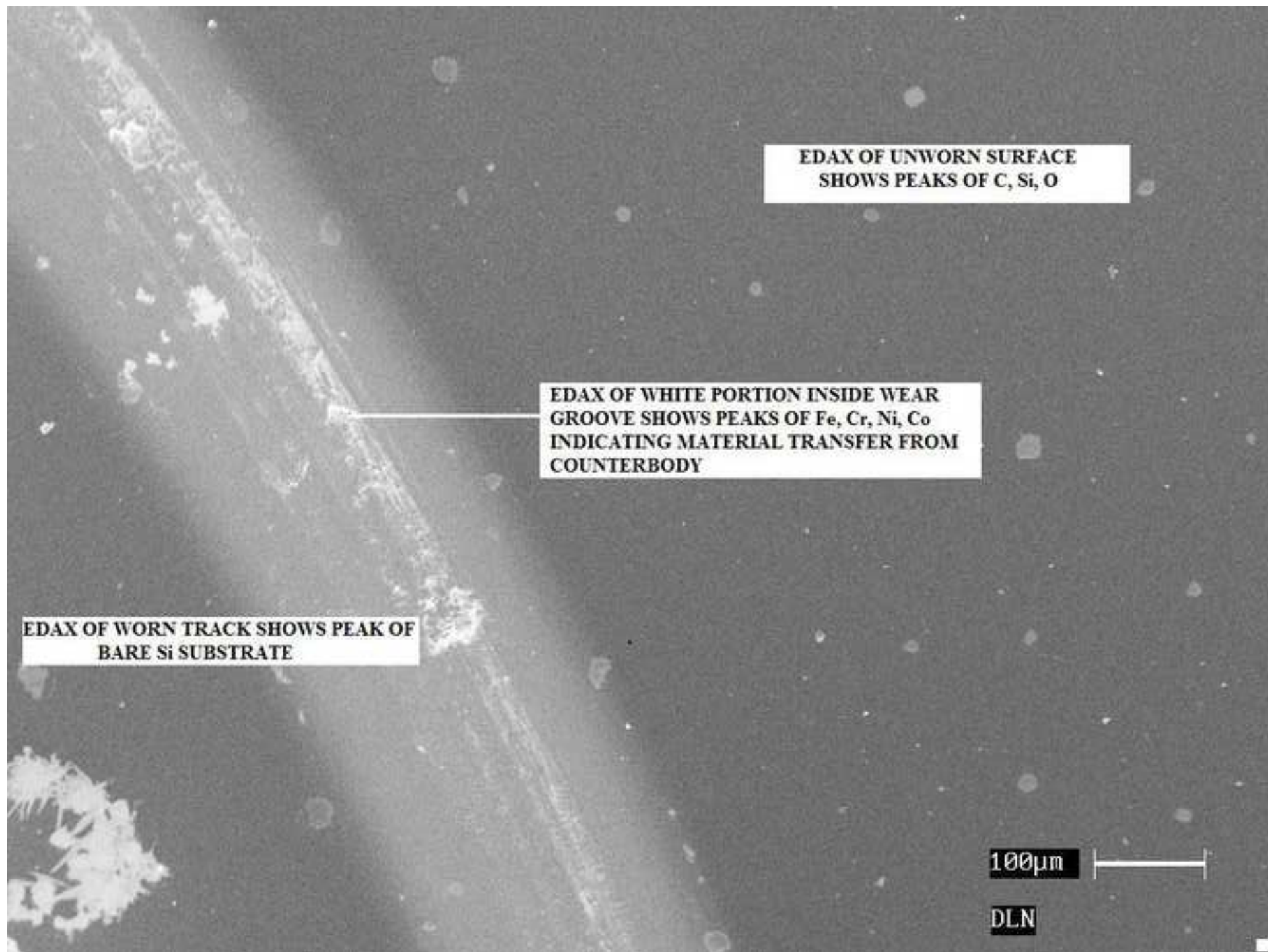


Figure 9
[Click here to download high resolution image](#)

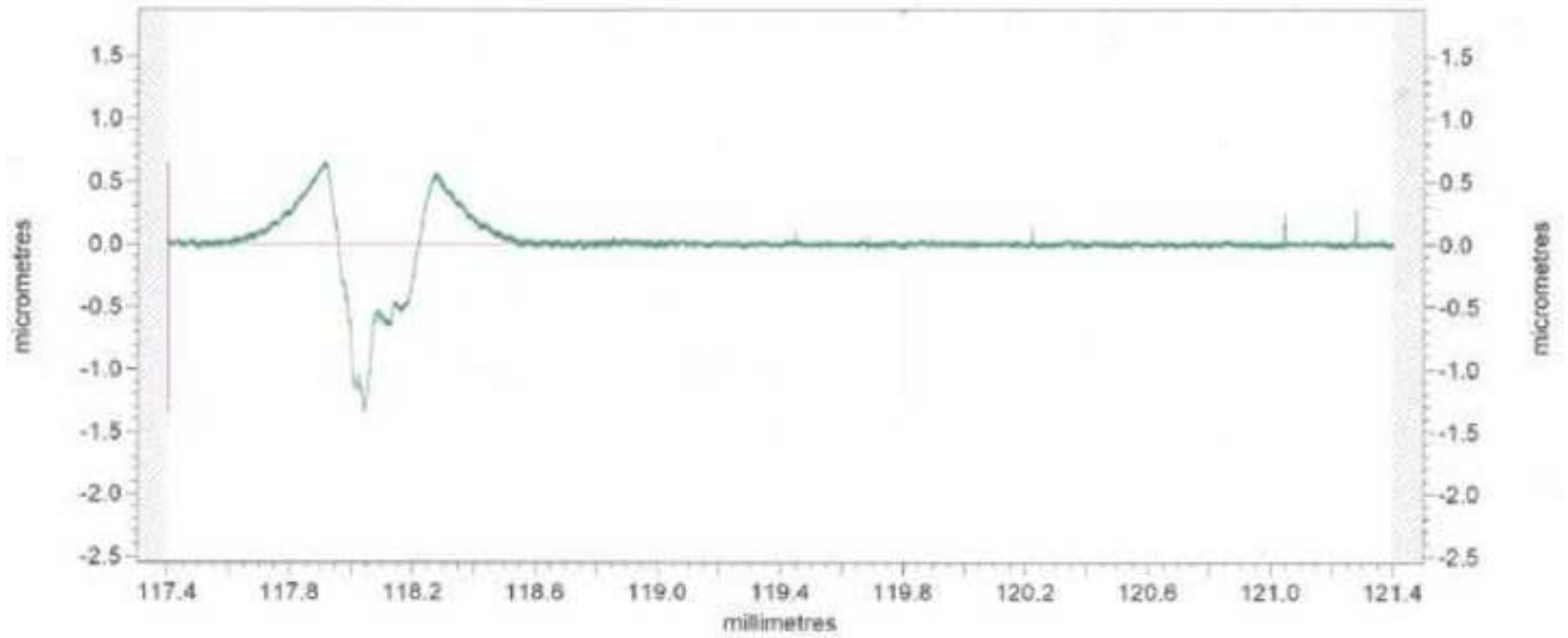


Figure 10
[Click here to download high resolution image](#)



**UNCOATED FEMORAL
COMPONENT OF KNEE
IMPLANTS**



**DLN COATED FEMORAL
COMPONENT OF KNEE
IMPLANTS**

Table 1. Comparison of properties among diamond, diamond like carbon (DLC) and diamond like nanocomposite (DLN) coatings.

Properties	Diamond	DLC	DLN
Resistivity (Ω cm)	$>10^{16}$	10^{10} - 10^{13}	10^{-4} - 10^{14}
Hardness (GPa)	90	10-32	10-22
Coefficient of Friction (against Steel)	-	0.1-0.2	0.03-0.2
Wear Factor (10^{-7} mm ³ /Nm)	-	0.5-1	0.2 – 0.4
Transmission	UV-VIS-IR	VIS-IR	VIS-FAR IR
Modulus of Elasticity (GPa)	1145	100-340	150-200
Residual Stress	Almost nil	8-10GPa	200-300 MPa
Dielectric Constant	-	-	3-9
Maximum Operating Temperature ($^{\circ}$ C)	-	300	600 (O ₂ atm) 1200 (O ₂ free)

Table 2. PECVD Deposition conditions

Substrates	Precursor Flow rate (ml/10min)	Time of Deposition (min)	Total Precursor Used (ml.)	Bias Voltage (V)	Plasma Current (A)	Base Pressure (mbar)
SS 316L	1.7522	100	19.09	550	0.8	1×10^{-4}
Ti6Al4V alloy and Co-Cr alloy	1.3831	127	17.57	600	0.8	9.5×10^{-5}
UHMWPE and Glass	1.0199	29	2.96	600	0.8	9.6×10^{-5}
Acetabular cup	0.8863	65	5.761	700	0.8	1×10^{-4}
Co-Cr alloy based Knee implant	1.6526	93	15.371	700	0.8	5×10^{-5}

Table 3: Gaussian analyses of Raman spectra deconvoluted into D and G peaks in DLN films coated in different substrates (ν : position, Γ : Full Width at Half Maxima, I : Integrated intensity)

Substrate	ν_D (cm ⁻¹)	Γ_D (cm ⁻¹)	ν_G (cm ⁻¹)	Γ_G (cm ⁻¹)	I_D/I_G
CrCoMo alloy	1396.4	272.733	1536.91	156.493	1.53
Si(100)	1385.5	305.251	1533.94	146.974	2.05
SS 316L	1382.9	300.112	1529.08	145.306	2.19
Ti6Al4V alloy	1390.78	304.394	1541.07	138.599	2.71

Table 4. Mechanical Properties of DLN coatings

Sample	Roughness Ra (μm)	Thickness (μm)	Hardness GPa	Young's Modulus GPa	Critical Load L_C (N) with standard deviation
DLN on SS 316 L substrates	0.1003 (bare) 0.1466 (coated)	1.75	17	132	0.618 ± 0.004
DLN on Glass substrates	<i>Very smooth</i> before and after coating	0.66	14	73	0.196 ± 0.023

Table 5. Wear and Friction data of steel ball sliding against DLN coated silicon substrate

Temperature °C	No. of revolutions	Wear (mm³/N.m)	Co-efficient of friction
28.8	90000	1.26 E-7	0.043
30.4	110000	1.33 E-7	0.092
28.4	150000	1.79 E-7	0.143